Steel and Composite Structures, *Vol. 20, No. 3 (2016) 671-692*
DOI: http://dx.doi.org/10.12989/scs.2016.20.3.671

Bond between FRP formworks and concrete-effect of surface treatments and adhesives

Reema Goyal [1], Abhijit Mukherjee[*2] and Shweta Goyal [1]

[1] *Department of Civil Engineering, Thapar University, Patiala 147001, India*
[2] *Department of Civil Engineering, Curtin University, Perth, WA 6102, Australia*

(*Received September 12, 2015, Revised November 12, 2015, Accepted December 01, 2015*)

Abstract. FRP stay-in-place (SIP) formworks are designed as a support for casting concrete and as a tension reinforcement when concrete is cured. Bond development between SIP formwork and concrete is critical for FRP tension element to be effective. This paper reports the bond strength between FRP formwork and concrete for different interfacial treatments. A novel experimental setup is prepared for observing the bond behaviour. Three different adhesives with varying workability have been investigated. Along with the load-deformation characteristics, bond slip and strains in the formwork have been measured. A finite element numerical simulation was conducted for the experiments to understand the underlying mechanism. The results show that the adhesive bonding has the best bond strength.

Keywords: Fibre Reinforced Polymers (FRP); bond; adhesives; aggregate bonding; adhesive bonding; failure modes

1. Introduction

Fibre reinforced polymers (FRP) are transcending from a niche material to mainstream in the construction industry. Last two decades of research has established its efficiency in enhancement of bending and shear (Mukherjee and Joshi 2005, Mukherjee *et al*. 2009) capacities of flexure elements and improving confinement of concrete in compression elements (Mukherjee *et al*. 2004). Successful experimental designs and numerical models for improving the performance of concrete beam-column joints under cyclic loads have been reported (Mukherjee and Jain 2013). Their durability in the tropical climate of India is also demonstrated (Mukherjee and Arwikar 2005a, b, Mukherjee and Arwikar 2007a, b). As a result, FRP is the material of choice in seismic retrofits of structures. In these applications FRP sheets or laminates are bonded externally on concrete surface. More recently, FRP pultruded sections such as rods and gratings have been used in new construction (Bakis *et al*. 2002, Mukherjee and Arwikar 2005a, b, Wang and Belarbi 2005). Progress in these fields has led to the concept of FRP structural stay-in-place (SIP) formwork systems. SIP formwork is a permanent participating system which is structurally integrated with the concrete. It has two roles: (1) it acts as a formwork at the time of casting of concrete; and (2) it becomes a reinforcement for the cured concrete. Nelson *et al*. (2014) observe that in case of bridge

*Corresponding author, Professor, E-mail: abhijit. mukherjee@curtin. edu. au

http://www. techno-press.org/?journal=scs&subpage=6 ISSN: 1229-9367 (Print), 1598-6233 (Online)

decks SIP can reduce 55% work of shuttering and further reduction in time and cost of reinforcement placement. They point out limitations of SIP as inaccessibility of concrete for inspection, unfamiliarity of contractors and cost. Moreover, fire susceptibility of FRPs is another concern. Another significant advantage of SIPs in case of buildings is that they can be fabricated with decorative finishes, thus eliminating the surface finishing works such as plastering and painting.

Broadly, SIP formworks are of two types: (1) SIP encasing concrete (Fam and Rizkalla 2001); and (2) SIP supporting concrete from the bottom. This study is restricted to SIP of the second type. Such a SIP made of corrugated steel has been used for quite a long time (Wright *et al*. 1987). However, corrosion of steel can be eliminated using FRP. In addition, FRP SIPs are lighter. They can be ideal material for permanent formworks provided they are made safe against high temperature and fire. Pultruded FRP panels with a flat continuous base and two T-up stands as shear studs have been tested as SIP (Hall and Mottram 1998). In Salem Avenue bridge deck project in Dayton, Ohio (Reising *et al*. 2004) and in Waupun, Wisconsin (Berg *et al*. 2006), FRP SIP was adopted. The exercise demonstrated that a 57% saving in labour costs was achieved in comparison to steel-reinforced decks, but the material cost was 60% higher. A rapid replacement of bridge deck in Missouri was completed with the use of a large scale structural FRP SIP form panel (Matta *et al*. 2006).

Prior research amply demonstrates the structural advantage of hybrid FRP-concrete composite construction where each material is optimally used; concrete in compression and FRP in tension (Hall and Mottram 1998, Dieter *et al*. 2002, Cheng *et al*. 2005, Ringelstetter *et al*. 2006, Bank *et al*. 2007, Keller *et al*. 2007, Honickman and Fam 2009). For the composite action it is essential to ensure bond between the prefabricated FRP and cast-in-place concrete after the setting of concrete. The bond between FRP and concrete can be achieved by a combination of good adhesion between the two materials and increasing the contact surface by profiling the FRP formwork. Good bond between FRP and concrete is a generic requirement for all applications and it is a well investigated research area. However, most of these investigations are on pullout properties of FRP adhesively bonded with cured concrete (Wu and Yin 2003, Teng and Lam 2004, Ueda and Dai 2005).

In case of SIP the concrete is poured on the formwork. Thus, the polymerisation happens between the adhesive and the fresh concrete. In some cases the formwork is first prepared with adhesively bonding one of the aggregates of concrete (coarse sand) prior to pouring concrete. Thus, there is a polymeric bond between FRP and the aggregate, while the concrete and the aggregate are bonded mechanically. In this paper we call this system *aggregate bonding*. Aggregate bonding essentially introduces two interfaces, one between the FRP and sand and the other between the sand and fresh concrete. Some guidelines for aggregate bonding are available from prior research. Importance of uniform coverage of aggregates on the SIP is emphasised (Dieter 2002). Smaller size aggregates with high distribution density has been found to give better shear bonding (Cho *et al*. 2010). It is also observed that shear bond of sand coated surface treatment was better than that of cross bars penetrated through the T stiffeners (He *et al*. 2012). Experiments of Bank *et al*. (2007) concluded that the FRP planks with epoxy bonded aggregate coating performed better than the steel reinforcements in terms of initial cracking moment capacity, ability to distribute flexural cracks and ultimate load carrying capacity.

It is also possible to apply the adhesive on the formwork and pour the concrete directly over it. We call this system *adhesive bonding* as a polymeric bond between the FRP and concrete is developed and the additional interface with mechanical bonding is dispensed with. Hall and Mottram (1998) conducted a push out test to compare bond performance of uncoated and epoxy coated I shaped FRP bars embedded in cast-in-place concrete and found that there is considerable increase in ultimate bond strength with epoxy coating. In coated bars the failure mode moved from the concrete-FRP interface to inside concrete failure. In the flexural tests of hybrid FRP-concrete bridge deck panels, 104% increase in load capacity was achieved through adhesive bonding (Keller *et al*. 2007). However, the failure mode changed from ductile to brittle. Fam and Nelson (2012) on the other hand reported that epoxy coating on corrugated plates used as SIP formwork resulted in significant enhancement of stiffness but very little gain in ultimate strength. Nelson *et al*. (2013) concluded that adhesive bonding at FRP–concrete interface increased the deck strength and initial stiffness by 30% and 73%, respectively. However, performance of different adhesives have been found to vary greatly (Zhang *et al*. 2014). Li *et al*. (2010) observed that in case of adhesive bonding, presence of fresh concrete had no negative effect on the degree of curing of epoxy adhesives and it even gained higher glass transition temperature.

Investigations on the relative performance of aggregate bonding and adhesive bonding have reported mixed results. Some conclude that adhesive bonding has similar load carrying capacity as the aggregate bonding (Honickman 2008, Boles *et al*. 2014), while others observe that adhesive bonding had higher average bond strength than aggregate bonding (Cho *et al*. 2006). Zhang *et al*. (2015) reported that the specimens with aggregate coating in which concrete was poured after adhesive had hardened showed poor performance than those with adhesive coating. The wide variations in the conclusions is possibly due to non-standard test methods and variety of adhesive materials.

Evidently, research on SIP formwork is mainly focussed on bridge decks. However, there are a large number of shorter span culverts where such formworks can be used to greatly reduce the time of construction. The objective of this research is to develop a cost effective culvert system for spans up to 3 m. However, the mandate of such applications is to manage the cost to the level of a standard reinforced concrete culvert. The main cost in the FRP concrete system is the SIP formwork. To avoid additional cost of development of a special SIP or a bonding system a standard commercial product fabricated for shorter walkways (up to 1 m) has been used along with commercially available adhesives that are in regular use in the construction industry. Likewise, a standard concrete mix that is in regular use in culvert construction has been used. Prior research shows that the bond between the SIP and the concrete is paramount for such applications. In this paper, we investigate the bond between FRP and cast-in-place concrete with two objectives (a) to examine the commercially available adhesive resins for bonding; and (b) to compare adhesive bonding and aggregate bonding. Push out tests have been conducted to evaluate the bond properties. The motive was to keep test method as simple as possible, so that it could be easily used without any special test frames. Load–displacement, load-slip and load-strain curves have been obtained for comparison of the performance of various adhesives. Failure mechanisms were noted. Finally, a finite-element numerical simulation was conducted to capture the experimental phenomena.

2. Experimental investigation

In this experimental investigation a commercially available GFRP plank, normally used for short walkways, is selected as SIP. Different kinds of adhesive bonding were created by applying commercially available adhesives. Aggregate bonding was also created for each of the adhesive types by applying sand on the adhesives. Concrete was poured over the SIP and cured for the specified period. The samples were subjected to a compressive force that tends to push concrete out of the SIP resulting in a shear load on the concrete-SIP interface. The responses in terms of displacements and strains at different points have been observed until failure. The modes of failure have been noted.

2.1 Materials

The FRP consisted of a portion of a commercially available pultruded GFRP plates with T-shaped ribs (Fig. 1). These planks are used for walkways in a span of 1 m. It is suitable as a SIP as longitudinal T ribs stiffen the plate so that the plank can bear the weight of fresh concrete. The ribs also offer mechanical anchorage with cured concrete. Separate samples of the plate and the stiffeners of the SIP were tested for tensile strength, Young's modulus and volume fraction according to ASTM D3039 and ASTM D 2584. The results are reported in Table 1. The tensile strength of the strips was found to be lower than the expected values for pultruded sections of the corresponding volume fractions. It is noted that facing layers of chop strand mat (CSM) have been used in the SIP that may not have contributed to the strength but it has been counted in the volume fraction. The variations in the strength are within the acceptable limits. The thickness of the stiffeners was less than that of the plate, but the thickness of the CSM sheet in both the plate and the stiffeners was the same. Thus, the proportion of CSM is higher in the stiffeners; and as a result, they have about 6% lower strength and 14% lower stiffness.

Commercially available adhesives were chosen keeping in mind their bond strength, ease of application, availability and economy. Manufacturer's specifications for their properties are in Table 2. Adhesives with longer pot life was considered to be easier to apply as they will allow

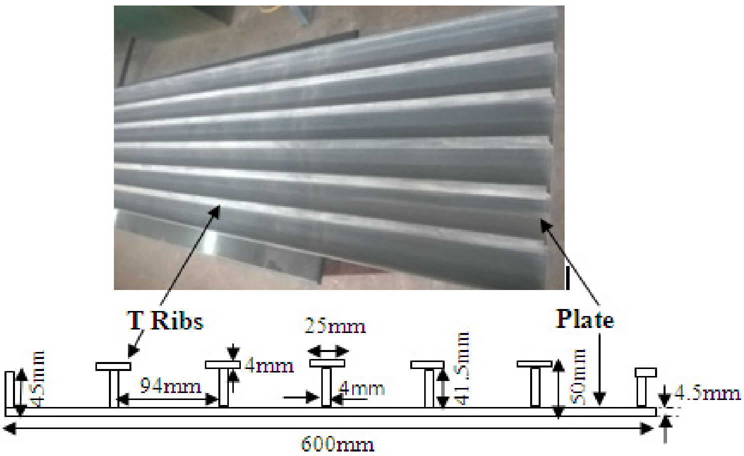

Fig. 1 The FRP plank

Table 1 Properties of GFRP profile

	Thickness (mm)	Tensile strength (MPa)		Young's Modulus (GPa)		Volume fraction
		Average	Std. Dev.	Average	Std. Dev.	
Plate	4. 5	375. 5	5. 86	27. 9	2. 55	0. 35
Stiffeners	4	352. 3	5. 45	23. 8	2. 2	0. 30

Table 2 Mechanical properties of the adhesives

Properties	Adhesive		
	A	B	C
Epoxy content	Two part epoxy	Three part epoxy	Two part epoxy
Pot life	120 min	30 min at 25°C	45 min at 25°C
Viscosity	Flowable (1000CPS at 25°C)	Viscous Thixotropic	Viscous Thixotropic
Glass transition temp.	65°C	62°C	Not available
E modulus	1. 27GPa	1. 1 GPa	5 GPa
Tensile strength	40MPa	45 MPa	15 MPa
Flexural strength	50 MPa	60 MPa	30 MPa
Bond strength	10. 3 MPa	Not available	8-10 MPa
Elongation at break	4. 5%	2. 2%	0. 4%
Cost (USD/Kg)	6. 24	6. 88	5. 31
Delivery (Days)	6	5	2

more time at site. A is an adhesive with low viscosity and flowable consistency. It also has a long pot life of 120 minutes. The longer pot life combined with flowable consistency would allow laying of concrete with ease. B is an epoxy based structural adhesive used for structural bonding of GFRP plates to concrete substrates. Its pot life is 30 minutes at 25°C. C is another two part epoxy resin system that according to the manufacturers is solvent-free, moisture tolerant and thixotropic with a pot life of 45 minutes at 25°C. It is noted that according to the manufacturers' data sheet the elastic modulus of C is claimed to be much higher than that in A and B. High variability of manufacturers' data was also reported earlier (Chajes *et al*. 1996, Shield *et al*. 2005, Zhang *et al*. 2014). In an investigation on near surface mounted FRP, Shield *et al*. (2005) report that even with adhesives of similar tensile strength and shear strength the bond strength and bond failure mechanism can differ significantly. Thus, it is important to evaluate the adhesives for the specific purpose. The cost and delivery period of all the adhesives were obtained (Table 2) to have an assessment of their commercial acceptability. It is observe that adhesive C has marginally lower cost and faster delivery mainly due to higher volume of usage and wide dealer network.

Self compacting concrete of 50 MPa strength was used and all samples were cast using the same batch of concrete to maintain low tolerance levels in the specimens. Self compaction was used to ensure uniform flow of concrete underneath the T-stiffeners without having to vibrate the concrete. The mass ratio of the concrete mix was 1 (cement): 0. 43 (water): 1. 5 (fine aggregate): 0. 94 (coarse aggregate with maximum size 10 mm): 0. 015 (water-reducing agent). A sulphonated naphthalene polymers based admixture was used as the water reducing admixture. In the workability test a slump flow diameter 600 mm was achieved.

2.2 Sample preparation

The GFRP planks have been cut to U shape consisting of the base plate and two stiffeners at the two sides (Fig. 2(a)). The length of the sample was 300 mm and width 120 mm. It was used as a formwork for casting concrete. The stiffeners served the purpose of two side forms. Steel plates were placed at the ends of the formwork as shown in Fig. 2, such that concrete could be cast for a

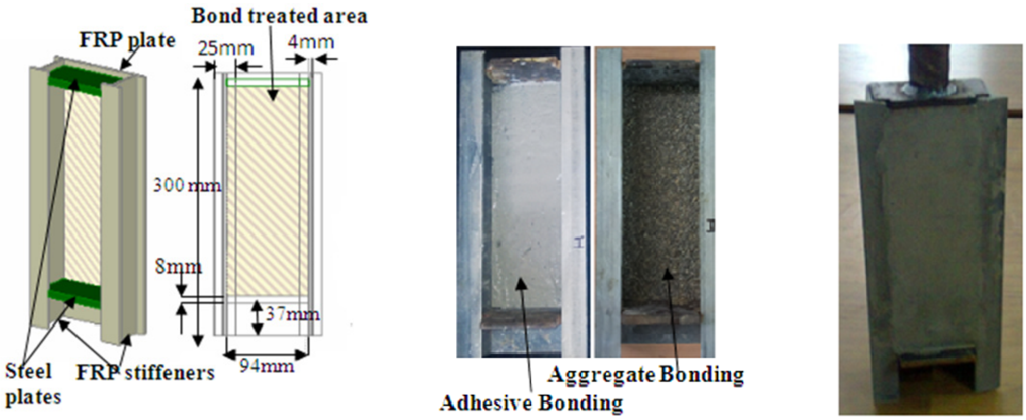

(a) Schematic diagram (b) Coatings (c) Cast samples

Fig. 2 Specimen details

length of 240 mm leaving a distance of 15 mm from top and 45 mm from bottom. Thereafter, bonding coats were applied on the surface of the plate only leaving the stiffeners uncoated (Fig. 2(b)). Two types of bonding were applied, aggregate bonding and adhesive bonding. In adhesive bonding a thin layer of the adhesive was applied directly on the plate without roughening or sanding. After about 10 minutes concrete was poured over the adhesive. This was well within the pot life period of the adhesive. In case of aggregate bonding the adhesive was applied on the surface of the plate. Sand aggregates were sieved to obtain size between 1.18 and 2.36 mm. The grains were evenly scattered over the entire surface of the wet adhesive and lightly pressed. The adhesive was allowed to cure for two days and by that time it hardened completely. The loose aggregates were removed by brushing. It may be noted that the bond treatment was applied only on the plate and the stiffeners were left untreated. Concrete was cast in the formwork and cured for 28 days.

Table 3 Specimen summary and load capacity

Series	Bond type (coating)	Adhesive used	Failure load (KN)	Failure mode
C	-	-	5	FRP-concrete interface failure
AA120	Adhesive	A	40. 5	FRP-adhesive interface failure
GA120	Aggregate	A	22	FRP-adhesive interface failure
AB30	Adhesive	B	73. 7	Concrete-adhesive interface failure
GB30	Aggregate	B	65	Midway between FRP-adhesive and concrete-adhesive interface failure
AC45	Adhesive	C	102	Concrete failure
*AC45-B			86	FRP buckling failure
GC45	Aggregate	C	75	Concrete –adhesive interface failure

* specimen in AC45 series in which failure occurred due to buckling

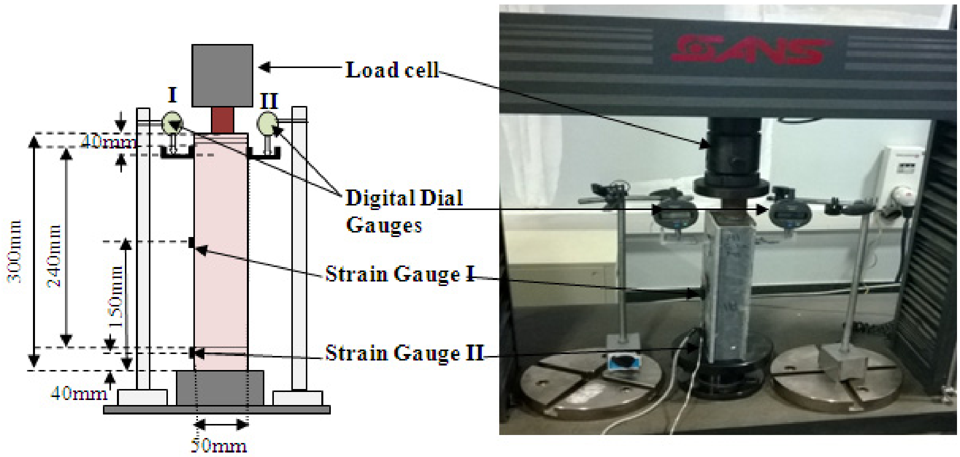

(a) Schematic view (b) Photographic image

Fig. 3 Test set up details

Table 3 illustrates the specimen details. The first row is for control samples with no bonding, shown as C. For the bonded samples the first letter of the nomenclature scheme is the bond type A for adhesive bonding and G for aggregate bonding. The second letter is for the adhesive type (A, B or C). The number following the second letter indicates the pot life of the adhesive in minutes. Thus, AA120 means the sample had adhesive bonding of type A that has a pot life of 120 mins. Five specimens for each adhesive type and bond type were prepared.

2.3 Experimental setup

Each specimen was positioned vertically in a universal testing machine (UTM) with the FRP end at the bottom and the concrete at the top (Fig. 4) and subjected to compression. At the top end of the specimen a steel plate with a bar welded to it was positioned to cover the entire concrete surface but no part of the plate was on the formwork. Thus, only concrete was loaded with uniform compression at top. The other end of the sample rested on the loading plate of the UTM. Thus, the sample was loaded fully through the FRP formwork at the bottom. The entire force transfers through the bonded FRP-concrete interface as shear. Each specimen was subjected to compression and their displacement, load capacity, failure mode, interfacial slip, and strain distribution at different locations of the FRP plate were recorded. All specimens were tested in displacement control mode with rate of loading 0.2 mm/min. Two digital dial gauges were positioned at a distance of 40 mm from top to record the movement of the outside surfaces of FRP and concrete. While one dial gauge (Dial gauge I) monitored the displacement of FRP, the second dial gauge (Dial gauge II) monitored displacement of concrete. The difference between the two dial gauge readings was considered the slip between concrete and FRP. FRP strain distribution was measured for two specimens of each type. To measure the strain distribution along the FRP, two strain gauges of gauge length 5mm were attached along the centre line of FRP plate at the distance of 35 mm and 150 mm from the base.

3. Experimental results

3.1 Failure modes

The failure mode and ultimate load carrying capacity of all sets of specimens is presented in Table 3. There were three components in the specimens- concrete, FRP and the interface between them. Failure took place when any one of these components had failed.

3.1.1 Interface failure

The images of the failed samples with interface failure are in Figs. 4 and 5. In case of the control sample no treatment to bond FRP with concrete was applied. In this case with slipped out of the mould as a wedge with no trace of concrete left on the FRP (Fig. 4(a)). The failure took place at 5 kN. This result clearly exhibits that the FRP and the concrete do not bond with each other on their own. A treatment of the interface is essential to improve the bond between them.

When the interface was treated the failure loads increased substantially. However, the interface failure was still observed in some samples depending on the strength of the bond. In the bonded samples there was an additional bonding layer between the FRP and the concrete. Thus, the interface between the bonding layer and the concrete could fail. Alternatively, the interface between the FRP and the bonding layer could also fail. Both types of failures were observed in the tests. In case of the failure at the FRP-adhesive interface a clean surface of the FRP with almost no trace of the adhesive was obtained, while the adhesive stuck to the concrete. Such failures happened suddenly with a loud noise. All specimens with A type adhesive (both GA120 and AA120 series) failed due to FRP-adhesive interface failure (Figs. 4(b) and (c)). Clearly, although it bonds with concrete, adhesive A does not bond with the FRP well. It is unsuitable for concrete-FRP bonding. In this case, some specimens had small patches of concrete at the corners of the FRP. This indicates some concrete cracking at the corners. When we performed the finite element analysis of the samples the stress plots show high stress concentration at the corners. In adhesive A specimens with aggregate bonding failed at a relatively low load of around 22 KN. In case of adhesive bonding, in comparison, a failure load of around 40 KN was observed. It may be noted

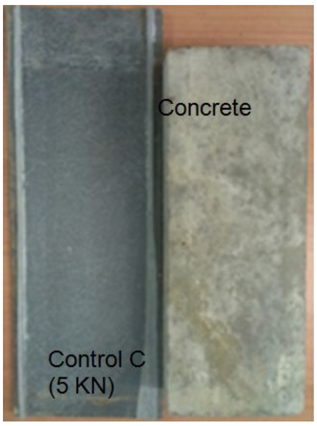

(a) Control C

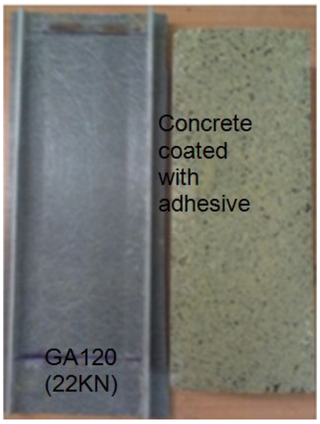

(b) GA120

(c) AA120

Fig. 4 Specimens with FRP-adhesive interface failure

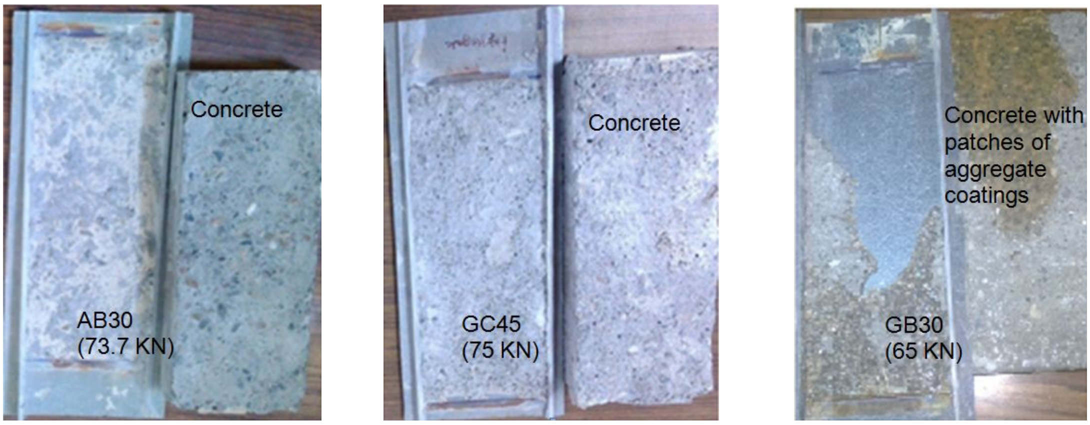

(a) AB30 (b) GC45 (c) GB30

Fig. 5 Specimens with concrete- adhesive interface failure

that the adhesive A has the lowest viscosity and flows easily. Thus, it may have created a thinner adhesive layer and the sand grains were not securely bonded with the FRP. Thus it resulted in a poor interfacial bond. In case of adhesive bonding due to the higher pot life and flowable consistency of adhesive A when wet concrete was poured over it some of the adhesive floated up leaving the concrete-FRP interface. Thus, a weaker interface was created.

When the bond between the adhesive and the FRP was strong enough the failure plane shifted to the concrete-adhesive interface. A thin layer of the cement paste and fine aggregates was attached to the FRP. Large aggregates were rarely attached to the FRP. The failure started with a few sounds of cracking and the final one was sudden with a loud noise. This mode of failure was noticedGC45 (Fig. 5(a)) and AB30 (Fig. 5(b)). In some cases a mixed mode failure where in part the adhesive-concrete interface and in part the adhesive-FRP interface failed. GB30 in Fig. 5(c) is an example. The capacity of both AB and GB specimens was much higher than that of Adhesive A specimens. The adhesive bonded specimens (73.5 KN) had 12% higher average load capacity than the aggregate bonded specimens (65 KN).

3.1.2 Material failure

Specimens with Adhesive C exhibited failure either in concrete or in FRP. Thus, the limit of interfacial bond strength was reached with Adhesive C. Any further increase in the load capacity of the specimens would necessitate increase in strength of the constituent materials. In case of concrete failure, the load increased smoothly up to about 70% of failure load. Low intensity cracking sounds started sporadically and became more frequent as the failure load approached. The specimen failed with a loud noise. Cracks passed through the concrete and often disintegrated it. A thick layer of concrete remained attached to the FRP (Fig. 6(a)). In this case large aggregates were clearly visible in the attached layer. Thus, the cracks went through the aggregates. With this mode of failure we reached the capacity limit of the specimens. To carry any further load beyond this point concrete strength will have to be improved.

In some samples the delamination in the FRP plate and consequent local buckling was observed (Fig. 6(b)). It initiated in the bottom portion of the samples in the area between the loading platen

(a) AC45 (b) AC 45-B

Fig. 6 Specimens with material failure-concrete failure and buckling failure

and concrete. In this zone FRP carries all the load in compression. Thus, buckling of FRP occurs in samples where the layers of FRP delaminate. Continuous cracking noise was heard throughout the buckling period. Sometimes the plate separated from the stiffeners and sometimes the layers of the plate delaminated. In the areas of delamination lack of enough adhesive was observed. Evidently, the quality of the commercial FRP formwork is not uniform. In these specimens the failure load of concrete was not reached. Buckling resulted in bending-tension pull in concrete. Ultimately, concrete split horizontally at failure. However, these samples carried at least 80% of the load at which concrete had failed. Thus, this defect in FRP does not reduce the capacity of the specimens by a large extent. Moreover, for the present application FRP is used as the tension reinforcement. Therefore, compression force is not envisaged in it.

Samples with adhesive C had the highest load capacities, with the adhesively bonded samples reaching 102 kN. In this case the load capacity of the adhesively bonded samples was 15 to 30% more than that in aggregate bonded samples. Table 3 shows that the bond strength between FRP and concrete can greatly vary depending on the type of adhesive and the surface treatment. It demonstrates that a bond treatment at the concrete-FRP interface is essential for SIP formworks. The high pot life adhesives (type A) may not bond well with FRP. Therefore, we may have to sacrifice pot life of the adhesive to achieve adequate bond strength. However, commercially available epoxy adhesives (type C) are able to provide enough bond strength to cause material failure in concrete of compressive strength 50MPa. In our investigation the adhesive bonding achieved higher bond strength than aggregate bonding. Adhesive bonding obviates the necessity of aggregate coating. Thus, it is also faster and convenient to apply.

When we compare adhesives B and C in Table 2 we note that the properties as have been claimed by the manufacturers vary greatly. However, the performance of specimens with adhesives B and C in our tests is not significantly different. This may be due to different methods of testing the adhesives adopted by different manufacturers. The results demonstrate the perils of choosing adhesives based on manufacturer's data and emphasise the importance of conducting one's own tests. It indicates that other material properties such as ultimate shear strain and shear modulus of adhesive may play an important role in determining the amount of bond that can be developed.

3.2 Load displacement behaviour

Fig. 7 shows the load–v_c (concrete displacement measured by digital dial gauge II) plots for the different systems. The mean curve has been plotted and the standard deviation has been presented in the form of error bars. The curves have been grouped according to the mode of failure. All the plots show nearly linear behaviour until the maximum load is reached and thereafter unload rapidly. The control specimen slipped readily and offered by far the lowest resistance. However, it continued to offer the same resistance. The treated samples offered far higher resistance. However, after the maximum force was reached the failure was sudden. The maximum load was reached at a displacement ranging from 0.8 mm to 1.5 mm. The control sample exhibited the lowest stiffness (Fig. 7(a)). The specimens with FRP-adhesive interface failure had nearly two times more stiffness than the control samples. The specimens with concrete-adhesive interface failure achieved about three times more stiffness than the samples failing through FRP-adhesive interface failure. Stiffness of specimens with material failure was similar to that of the ones with concrete-adhesive interface failure. However, their displacement at maximum load was about 10% higher. Clearly, the adhesive type influences the failure mode and the specimen stiffness.

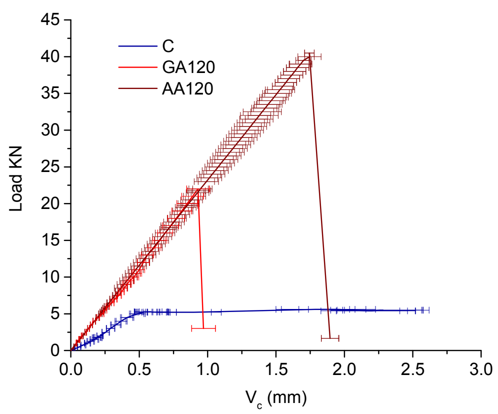

(a) FRP-adhesive interface failure

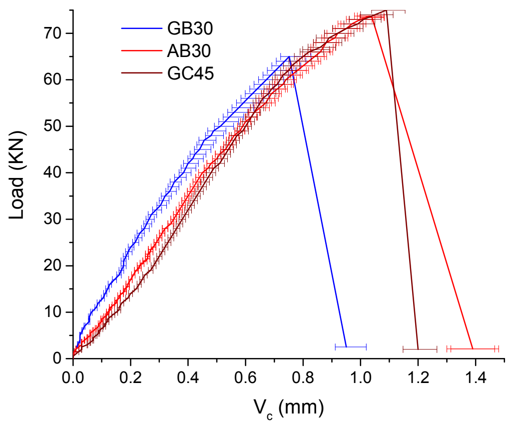

(b) Adhesive-concrete interface failure

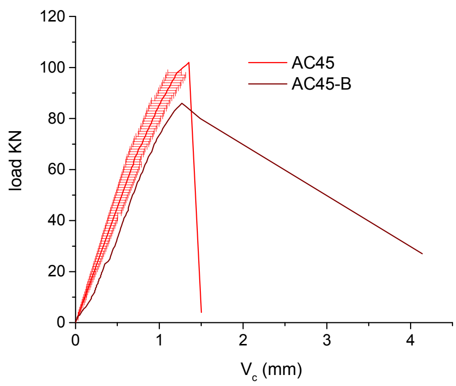

(c) Material failure

Fig. 7 Load-concrete displacement (v_c) plot for different failure modes

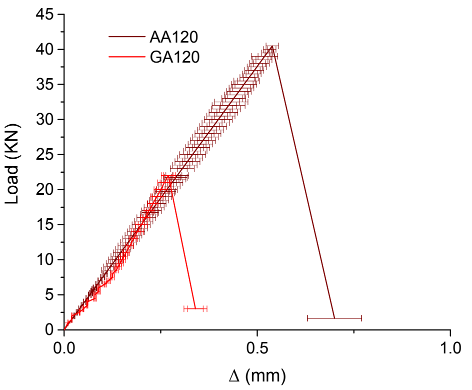

(a) FRP-adhesive interface failure

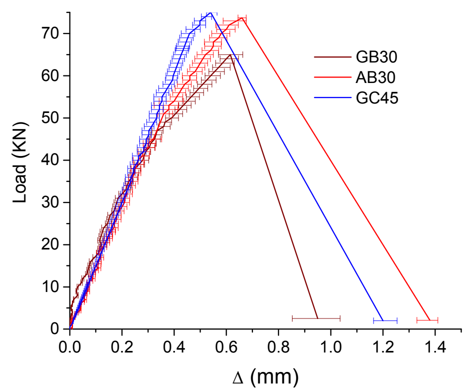

(b) Adhesive-concrete interface failure

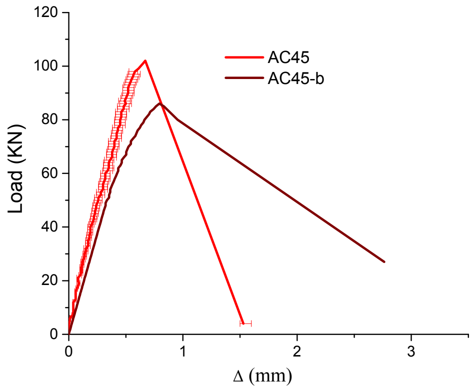

(c) Material failure

Fig. 8 Load-Δ plot for different failure modes

We investigate the interfacial slip behaviour of the specimens in Fig. 8. This is done by measuring the difference between the two dial gauge readings (Δ = Dial gauge II - Dial gauge I). Itmay be noted that dial gauge I is fitted on the FRP plate and dial gauge II is on concrete (Fig. 3). The difference between them is an estimate of the interfacial slip. Admittedly, the dial gauges are not located exactly at the slip plane. However, it is a reasonable estimate of slip. In this case too the samples exhibited near-linear behaviour until the maximum load is reached. They unloaded rapidly afterwards. Fig. 8(a) shows that the FRP-adhesive failure samples had slipped readily at a relatively low load. Concrete-adhesive failure samples had very similar slip characteristics (Fig. 8(b)). The slip stiffness in material failure samples was the highest (Fig. 8(c)). In this case when the failure is due to buckling of FRP the unloading is gradual. While concrete fails suddenly. The slip characteristics of adhesive bonding and aggregate bonding was similar.

3.3 Effect of bond length on bond stress

From the above investigation adhesive C was selected for further investigation. The experimental programme was extended to observe the effect of the bonded area on the strength of the sample. In addition to the previous experiments specimens of the same SIP of different lengths:

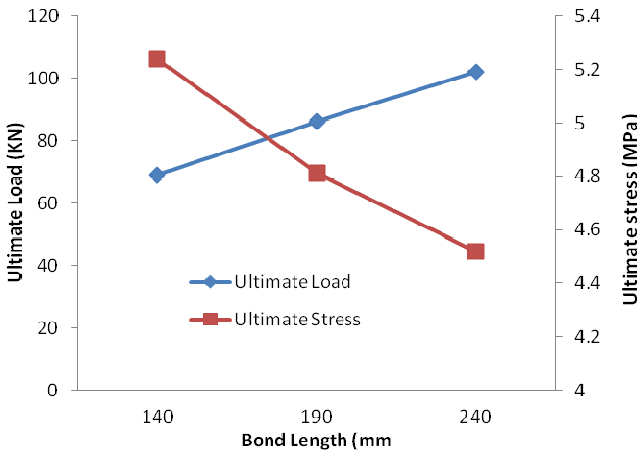

Fig. 9 Effect of bond length on ultimate load and ultimate stress

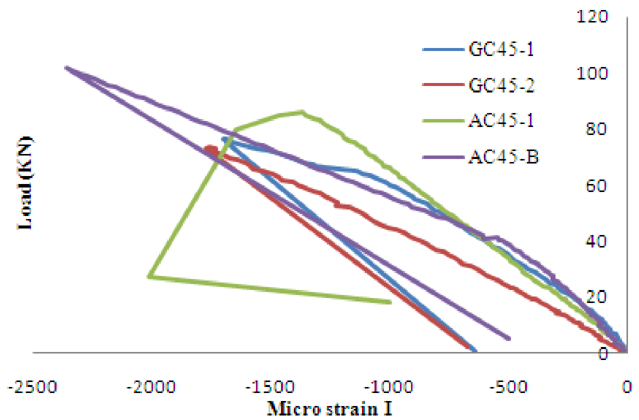

(a) Micro strain I

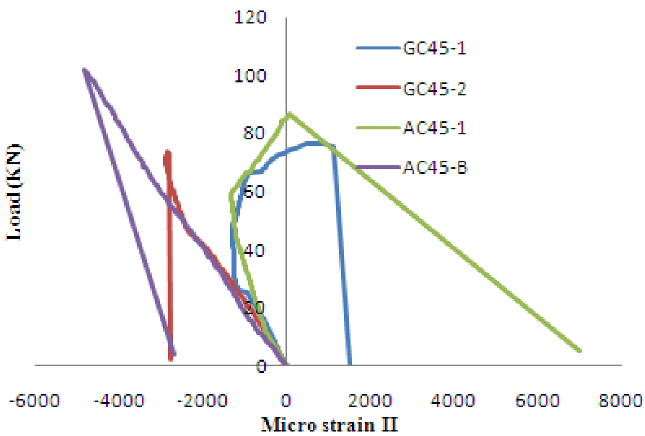

(b) Micro strain II

Fig. 10 Strains in FRP Plate at different locations

190 mm and 140 mm were prepared. From Fig. 9 it can be seen that the ultimate load of the samples increases with increasing bond length. However, the average shear stress decreases with increasing area of bond. It is due to the non-uniform distribution of shear stress in the bonded area that causes local failure. Also other modes of failure get initiated with the increasing area of bond. Brosens and Van Germet (1997) had similar observations regarding bond length in shear tests. Hosseini and Mostofinjad (2014) concluded that the ultimate load increases with increase in the length till the effective length is reached after which there is no increase in load with increase in length. In our experiment we have noticed that the increase in the failure load decreases with increase in bond length. Thus, it manifests the existence of an effective bond length.

3.4 Strain distribution in FRP

Strain was measured for 2 specimens of each series at the locations indicated in Fig. 3. The strains recorded in adhesive C specimens that had the highest load capacities, and largest strains, have been presented in Fig. 10. Strain1 is at 150 mm from the bottom, at the mid height of the specimen. Understandably, the strains are always compressive. They increase in almost linear fashion until the maximum load and then they unload sharply indicating sudden failure. Only in the case of the buckled sample the unloading is more gradual. The maximum strain is about 0. 0025 which is well within the maximum strain capacity of the FRP. Thus, no failure in the FRP is observed. Strain 2 is at 40 mm from the bottom of the specimens. Below this region there is no concrete. Thus, FRP carries the load alone. Therefore, the strains are higher at this region. Even in this region the maximum strains 0.0045 are within the limits of FRP. Interestingly, some samples have shown strain reversal and gone in the tension side. These are the samples where the FRP failed due to delamination and buckling. As a result, the FRP skin underwent bending resulting in tensile strains.

4. Finite element simulation

A finite element simulation of the experiment has been performed. It has been mentioned earlier that the performance of the adhesives did not correlate well with the manufacturer's specifications. To be able to design the full scale structure it is important to set the right parameters for the interface. The aim of the simulation is to have a better understanding of the interface characteristics and determine the interfacial properties that can be used in the full scale simulations. The best performing adhesive (type C) has been modelled using FEM.

4.1 Material and geometrical modelling

A three-dimensional finite element model using software ATENA was prepared to simulate the behaviour of the bond treated GFRP-concrete interface (Fig. 11). Table 4 shows all the properties used in ATENA for the constituent materials of the model. The 3D Nonlinear Cementitious 2 element was used for concrete. This fracture-plastic material model combines constitutive models for tensile (fracturing) and compressive (plastic) behaviour. Solid brick element having minimum 8 and maximum 20 nodes is taken for concrete elements. Two different mesh sizes were used for concrete modelling 10 mm and 8 mm, taking into consideration the aspect ratio.

The FRP formwork was modelled using 20 node quadratic 3D brick elements, specially used to model plate type structures, which has one dimension (thickness) very small compared to other

Table 4 Material properties for FEM analysis

Material	Material model in Atena	Important properties
Concrete	Nonlinear Cementious 2	F_{ck} = 50 MPa F_t = 4 MPa
Matrix	3D elastic isotropic	E = 3.5 GPa
Glass fibre	Reinforcement	E = 72 GPa
Steel	3D elastic isotropic	E = 200 GPa
FRP-concrete interface	3 D interface	$K_{nn} = 3\times10^5$ MN/m^3 $K_{tt} = 10^5$ MN/m^3 f_t = 15 MPa

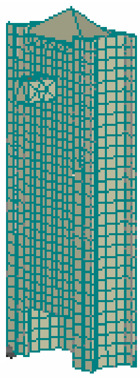

Fig. 11 FEM model

two. It accounts for both in-plane and bending stiffnesses. The FRP consists of two components: fibre and matrix. The fibre is embedded in the matrix. In the model, the fibre volume fraction of 35%, as observed in the experiment, was used. The matrix is defined as a 3D elastic isotropic material and glass fibres are defined as reinforcement. The shell element allows for different material layers with different constituents. Mesh size was taken to be 10 mm for the shell elements. To distribute the load evenly at the two ends of the model steel plates were used.

Modelling the bond between the concrete and the GFRP formwork is the most critical component. The 3D Interface element of ATENA was used to model bond between GFRP and concrete. In ATENA three contact types are available (1) perfect connection; (2) no connection; (3) contact element. The FE modelling of the interface involves defining a pair of surfaces located on both sides of the interface. In the original geometry the surfaces can share the same position or they can be separated by a quasi zero distance. The interface model is based on Mohr-Coulomb criterion with tension cut off. The constitutive relation for a general 3D case is given in terms of tractions on interface planes and relative sliding and opening displacements

$$\begin{Bmatrix} \tau_1 \\ \tau_2 \\ \sigma \end{Bmatrix} = \begin{pmatrix} K_{tt} & 0 & 0 \\ 0 & K_{tt} & 0 \\ 0 & 0 & \end{pmatrix} \begin{Bmatrix} \Delta v_1 \\ \Delta v_2 \\ \Delta u \end{Bmatrix} \tag{1}$$

where: τ is shear stress in direction x and y,

σ is normal stress,

Δv is relatively displacement in the interface plane,

Δu is displacement perpendicular to interface plain,

K_{tt} is initial elastic shear stiffness of the interface

K_{nn} is initial elastic normal stiffness of the interface

The initial failure surface corresponds to Mohr-Coulomb condition with tension cut off

$$\begin{gathered} \lfloor \tau \rfloor \le c + \sigma.\phi \quad \text{for} \quad \sigma < f_t, \\ \tau = 0 \quad \text{for} \quad \sigma > f_t \end{gathered} \tag{2}$$

Where, c is the cohesion of the interface.

ϕ is coefficient of friction;

f_t is tension strength on surface.

After stresses violate this condition, the failure surface collapses to a residual one which corresponds to the dry friction. In the model two sets of FRP-concrete interfaces were defined-untreated interface and bond treated interface. Untreated interface was used in the area where no bond treatment was applied at the FRP-concrete interface (between concrete and the stiffeners). Bond treatment was applied (between the plate and the concrete). It is important to set the normal and the tangential stiffness, cohesion and friction properties of the interface. For adhesive C, the elastic modulus of the fresh adhesive is reported as 5 GPa. In the present application concrete has been poured when the epoxy is not set. It has been reported that ingress of water reduces the modulus of epoxy (Wu *et al*. 2004). Based on that report the tangential and normal moduli of the interface was set at 100 GN/m^3 and 300 GN/m^3 respectively. The results have been compared with the perfect bond model where the interface does not deform at all.

4.2 FEM results and discussion

Fig. 12 shows comparison between load-concrete displacement and load-Δ obtained from experimental and FEM simulations both for the perfect bond and for the interface element. The tangential and secant stiffnesses of the perfect bond simulation are higher than the experimental observations almost through the entire load path. At close to failure the perfect bond sample loses its tangential stiffness rapidly. At failure its secant stiffness is very close to that observed in the experiment. Clearly, perfect bond overestimates the initial stiffness and underestimates the load capacity. As this model does not allow any deformation of the interface its stiffness is higher than that observed in the experiment. This result demonstrates that a deformable interface results in softer load-deflection behaviour. When the interface element was introduced in the model it followed the experimental curve more closely. The same trend was observed in case of the differential displacement curve. The simulation with interface element agreed with the experimental results more closely than the perfect bond.

While the stiffness of the model with perfect bond is higher than the experimental observations its load capacity is lower than that of the experimental result and interfacial element simulation. To investigate this point Von Mises stresses at the interface obtained from the two FE simulations have been plotted (Fig. 13) at the load level of 90 kN (the maximum load with perfect bond). Perfect bond leads to stress concentrations at the left and right edges of the concrete block. Thus, it resulted in an earlier failure of concrete. In case of the interfacial element simulation the resilience of the interface allows redistribution of the stresses and reduces the stress concentration. Thus, introduction of a flexible interface reduces the overall stiffness of the specimen, and increases its load capacity. The simulation with the interface element resulted in lower initial tangential and secant stiffnesses and it followed the experimental curve closely. The artefact of sudden drop in the tangential stiffness observed in case of perfect bond disappeared in the case of simulation with interface elements. This example emphasises the importance of a flexible concrete-FRP interface. To capture this phenomenon in the FE simulation inclusion of the interface element is essential.

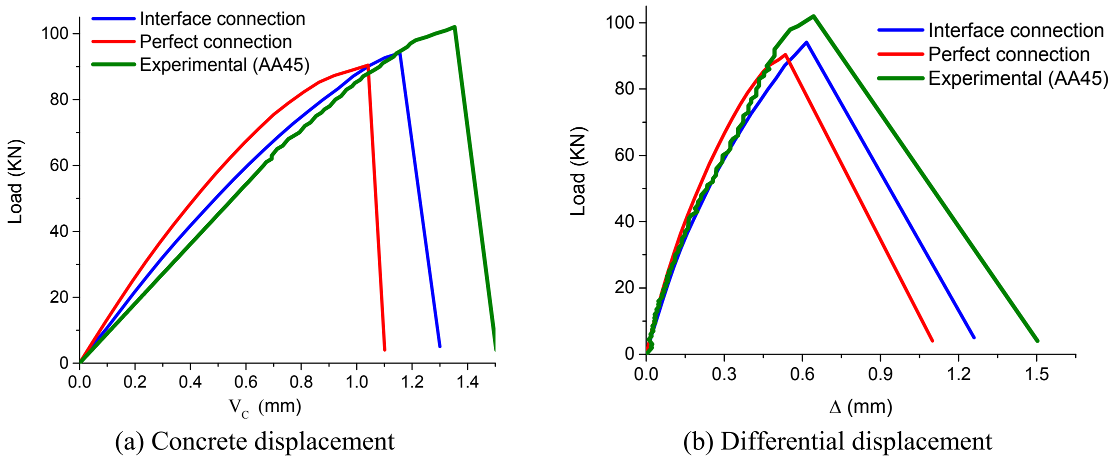

Fig. 12 Comparison between FEM results and experiment result

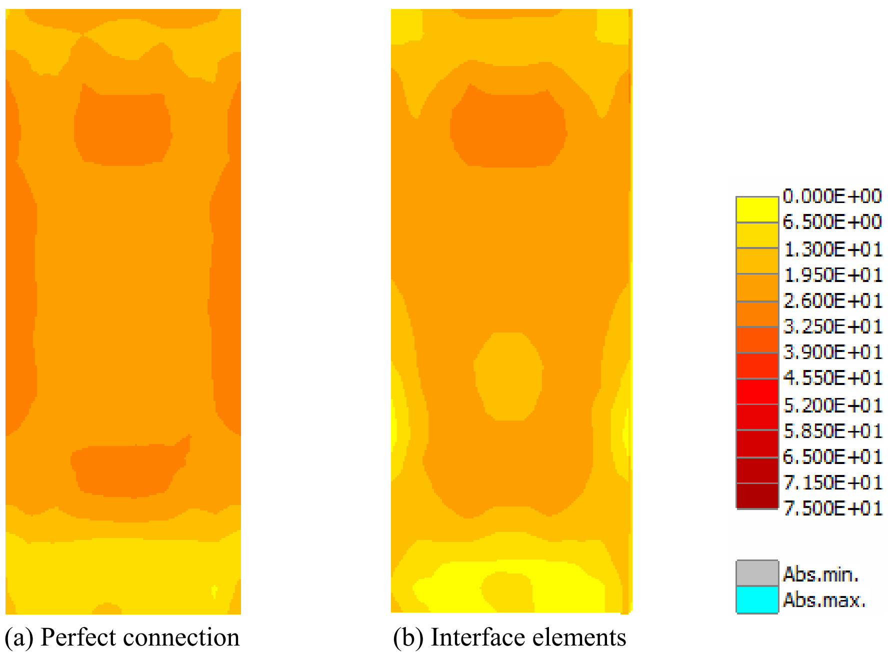

Fig. 13 Von Mises stresses at concrete interface

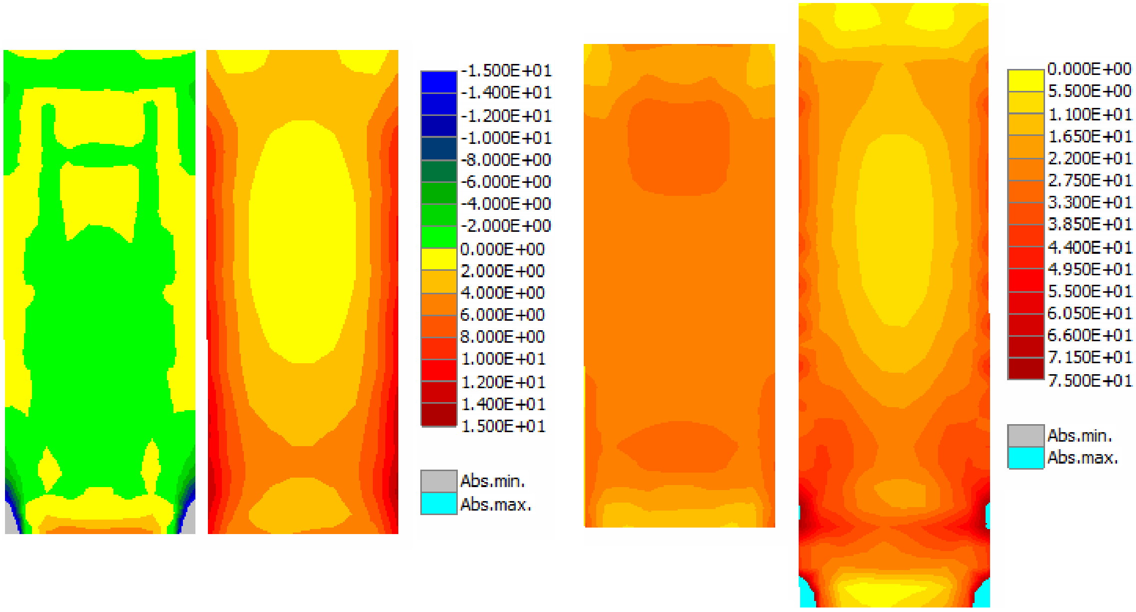

Interfacial stresses	Scale I	Von Mises stresses	Scale II
N	T1	Concrete	FRP

Fig. 14 Plot of normal stress and tangential stress at the interface (represented by scale 1) and von Mises stress for concrete and FRP plate (represented by scale 2) at ultimate load

Fig. 14 shows the tangential and the normal stresses at the interface along with the stresses in concrete and FRP when the load capacity has been reached for the interfacial strength 15 MPa. Clearly, the normal stress at the interface is low. However, the shear stress has reached the interfacial strength (15 MPa). At the same time, the stress in concrete has reached its limit (50 MPa). Thus, from this point onwards the failure shifts to the concrete. This is the limit interface strength. A stronger interface will not increase the load capacity unless the grade of concrete is improved.

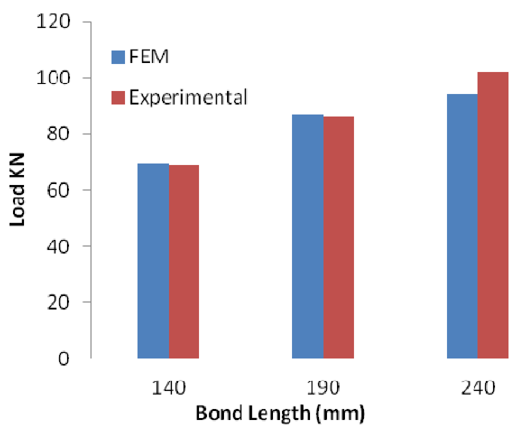

Fig. 15 Ultimate loads with varying bond lengths

Table 5 Effect of concrete strength

Interfacial strength (MPa)	Failure load at concrete compressive strength			
	30 MPa	40 MPa	50 MPa	60 MPa
I5	51.5 KN	50.8 KN	51 KN	50.9 KN
I15	73.5 KN	81.6 KN	KN	98 KN

To further examine the veracity of the model other experimental samples with different bond lengths were modelled in finite element. The experimentally observed load capacities have been compared with model predictions (Fig. 15). It can be seen that the model predicts the load capacity of different samples very close to that observed in the experiments.

The analysis with the present combination of concrete and interface treatment postulates that serendipitously an optimal combination of concrete and interface treatment was reached where both failed simultaneously. To examine this point a parametric study was carried out with varying concrete and interface properties. Four concrete strengths (30 MPa, 40 MPa, 50 MPa and 60 MPa) were investigated for two interfacial strengths (15 MPa and 5 MPa). Table 5 presents the estimated load capacities. It was found that in case of interfacial strength 5 MPa, there is no effect of concrete strength on the ultimate load as the failure occurs at the interface before the capacity of the concrete is reached. In case of interfacial strength 15 MPa, there is remarkable increase in the load capacity of the specimens was observed compared to the interfacial strength of 5 MPa for all types of concrete. Clearly, increase in the interface strength caused a shift in the failure from the interface to the concrete. Thus, as the concrete strength increased (second row) the laod capacity also increased with it. However, at the concrete strength of 50MPa the failure was simultaneous in the concrete and the interface. Thus, when the concrete strength increased to 60 MPa there was only a marginal increase in the load capacity of the specimen. Thus, the additional cost of producing 60 MPa concrete is not justified for the 15 MPa interface. It is evident that a concrete strength of 50 MPa and interfacial strength of 15 MPa is an optimal combination for the load capacity of the sample.

5. Conclusions

This paper investigates the interfaces between concrete and GFRP SIP formwork. To limit the cost of the system a commercially available pultruded plank has been used as formwork. Three different commercially available adhesive types have been investigated. Results of push out tests have been reported. The results show that the bond strength is heavily dependent on the choice of adhesive. Two different bonding techniques, adhesive bonding and aggregate bonding have been compared. The adhesive bonding is more convenient and performed marginally better than aggregate bonding. With adhesive bonding it was possible to shift the failure from the interface to concrete. Thus, a limit of interfacial strength was reached.

It is noted that adhesives with similar manufacturer's specifications perform differently. Thus, a finite element simulation has been performed to characterise the interface. The simulation demonstrated that in absence of an interface element in the model the stiffness is overpredicted and the load capacity is underpredicted. It also emphasises that a properly designed resilient interface can improve the load capacities by reducing stress concentrations. A limit in the interfacial strength is reached when the failure shifts to concrete. A parametric study by varying the strength of concrete demonstrated that a combination of interfacial strength and concrete strength can be reached for optimising the load capacity. The results will be used in the full scale numerical model and analytical tests that are presently underway.

Acknowledgments

The first author gratefully acknowledges the financial support provided by the Department of Science and Technology, India under women scientist scheme (WOS-A).

References

Bakis, C., Bank, L., Brown, V., Cosenza, E., Davalos, J., Lesko, J., Machida, A., Rizkalla, S. and Triantafillou, T. (2002), "Fiber-reinforced polymer composites for construction — State-of-the-art review", *J. Compos. Construct.*, **6**(2), 73-87.

Bank, L., Oliva, M., Bae, H.-U., Barker, J. and Yoo, S.-W. (2007), "Pultruded FRP plank as formwork and reinforcement for concrete members", *Adv. Struct. Eng.*, **10**(5), 525-535.

Berg, A.C., Bank, L.C., Oliva, M.G. and Russell, J.S. (2006), "Construction and cost analysis of an FRP reinforced concrete bridge deck", *Construct. Build. Mater.*, **20**(8), 515-526.

Boles, R., Nelson, M. and Fam, A. (2014), "Durability of bridge deck with FRP stay-in-place structural forms under freeze-thaw cycles", *J. Compos. Construct.*, **19**(4), 04014070.

Brosens, K. and Van Gemert, D. (1997), "Anchoring stresses between concrete and carbon fibre reinforced laminates", *Proceedings of International Conference on Composite Construction-Conventional and Innovative*, Innsbruck, Austria, September.

Chajes, M.J., Finch, W.W., Januszka, T.F. and Thomson, T.A. (1996), "Bond and force transfer of composite-material plates bonded to concrete", *Struct. J.*, **93**(2), 209-217.

Cheng, L., Zhao, L., Karbhari, V., Hegemier, G. and Seible, F. (2005), "Assessment of a steel-free fiber reinforced polymer-composite modular bridge system", *J. Struct. Eng.*, **131**(3), 498-506.

Cho, K., Cho, J.-R., Chin, W.-J. and Kim, B.-S. (2006), "Bond-slip model for coarse sand coated interface between FRP and concrete from optimization technique", *Comput. Struct.*, **84**(7), 439-449.

Cho, J.-R., Cho, K., Park, S.Y., Kim, S.T. and Kim, B.-S. (2010), "Bond characteristics of coarse sand coated interface between stay-in-place fibre-reinforced polymer formwork and concrete based on shear and tension tests", *Can. J. Civil Eng.*, **37**(5), 706-718.

Dieter, D.A. (2002), *Experimental and Analytical Study of Concrete Bridge Decks Constructed with FRP Stay-in-Place Forms and FRP Grid Reinforcing*, University of Wisconsin-Madison, Madison, WI, USA.

Dieter, D., Dietsche, J., Bank, L., Oliva, M. and Russell, J. (2002), "Concrete bridge decks constructed with fiber-reinforced polymer stay-in-place forms and grid reinforcing", *Transportation Research Record*: *J. Transport. Res. Board*, **1814**(26), 219-226.

Fam, A. and Nelson, M. (2012), "New bridge deck cast onto corrugated GFRP stay-in-place structural forms with interlocking connections", *J. Compos. Construct.*, **16**(1), 110-117.

Fam, A. and Rizkalla, S. (2001), "Behavior of axially loaded concrete-filled circular fiber-reinforced polymer tubes", *Struct. J.*, **98**(3), 280-289.

Hall, J. and Mottram, J. (1998), "Combined FRP reinforcement and permanent formwork for concrete members", *J. Compos. Construct.*, **2**(2), 78-86.

He, J., Liu, Y., Chen, A. and Dai, L. (2012), "Experimental investigation of movable hybrid GFRP and concrete bridge deck", *Construct. Build. Mater.*, **26**(1), 49-64.

Honickman, H.N. (2008), *Pultruded GFRP Sections as Stay-in-Place Structural Open Formwork for Concrete Slabs and Girders*, Queen's University Kingston, ON, Canada.

Honickman, H. and Fam, A. (2009), "Investigating a structural form system for concrete girders using commercially available GFRP sheet-pile sections", *J. Compos. Construct.*, **13**(5), 455-465.

Hosseini, A. and Mostofinejad, D. (2014), "Effective bond length of FRP-to-concrete adhesively-bonded joints: Experimental evaluation of existing models", *Int. J. Adhes. Adhes.*, **48**, 150-158.

Keller, T., Schaumann, E. and Vallée, T. (2007), "Flexural behavior of a hybrid FRP and lightweight concrete sandwich bridge deck", *Composites Part A: Appl. Sci. Manuf.*, **38**(3), 879-889.

Li, L., Shao, Y. and Wu, Z. (2010), "Durability of wet bond of hybrid laminates to cast-in-place concrete", *J. Compos. Construct.*, **14**(2), 209-216.

Matta, F., Nanni, A., Ringelstetter, T.E. and Bank, L.C. (2006), *Rapid Construction of Concrete Bridge Deck using Prefabricated FRP Reinforcement*.

Mukherjee, A. and Arwikar, S.J. (2005a), "Performance of glass fiber reinforced polymer rebars in tropical environment- II.Microstructural tests", *ACI Struct. J.*, **102**(6), 816-822.

Mukherjee, A. and Arwikar, S.J. (2005b), "Performance of gass fiber-reinforced polymer reinforcing bars in tropical environments - Part I: Structural scale tests", *ACI Struct. J.*, **102**(5), 745-753.

Mukherjee, A. and Arwikar, S.J. (2007a), "Performance of externally bonded GFRP sheets on concrete in tropical environments.Part I: Structural scale tests", *Compos. Struct.*, **81**(1), 21-32.

Mukherjee, A. and Arwikar, S.J. (2007b), "Performance of externally bonded GFRP sheets on concrete in tropical environments.Part II: Microstructural tests", *Compos. Struct.*, **81**(1), 33-40.

Mukherjee, A. and Jain, K. (2013), "A semi-analytical model of cyclic behavior of reinforced concrete joints rehabilitated with FRP", *Adv. Struct. Eng.*, **16**(12), 2019-2034.

Mukherjee, A. and Joshi, M. (2005), "FRPC reinforced concrete beam-column joints under cyclic excitation", *Compos. Struct.*, **70**(2), 185-199.

Mukherjee, A., Boothby, T., Bakis, C., Joshi, M. and Maitra, S. (2004), "Mechanical behavior of fiber-reinforced polymer-wrapped concrete columns — Complicating effects", *J. Compos. Construct.*, **8**(2), 97-103.

Mukherjee, A., Bagadi, S.P. and Rai, G.L. (2009), "Semianalytical modeling of concrete beams rehabilitated with externally prestressed composites", *J. Compos. Construct.*, **13**(2), 74-81.

Nelson, M., Eldridge, A. and Fam, A. (2013), "The effects of splices and bond on performance of bridge deck with FRP stay-in-place forms at various boundary conditions", *Eng. Struct.*, **56**, 509-516.

Nelson, M.S., Fam, A.Z., Busel, J.P., Bakis, C.E., Nanni, A., Bank, L.C., Henderson, M. and Hanus, J. (2014), "FRP stay-in-place structural forms for concrete bridge decks: A state-of-the-art review", *Struct. J.*, **111**(5).

Reising, R., Shahrooz, B., Hunt, V., Neumann, A. and Helmicki, A. (2004), "Performance comparison of four fiber-reinforced polymer deck panels", *J. Compos. Construct.*, **8**(3), 265-274.

Ringelstetter, T., Bank, L., Oliva, M., Russell, J., Matta, F. and Nanni, A. (2006), "Cost-effective, structural stay-in-place formwork system of fiber - Reinforced polymer for accelerated and durable bridge deck construction", *Transportation Research Record: J. Transport. Res. Board*, **1976**, 183-189.

Shield, C., French, C. and Milde, E. (2005), "The effect of adhesive type on the bond of NSM tape to concrete", *Special Publication*, **230**, 355-372.

Teng, J. and Lam, L. (2004), "Behavior and modeling of fiber reinforced polymer-confined concrete", *J. Struct. Eng.*, **130**(11), 1713-1723.

Ueda, T. and Dai, J. (2005), "Interface bond between FRP sheets and concrete substrates: properties, numerical modeling and roles in member behaviour", *Prog. Struct. Eng. Mater.*, **7**(1), 27-43.

Wang, H. and Belarbi, A. (2005), "Flexural behavior of fiber-reinforced-concrete beams reinforced with FRP rebars", *Special Publication*, **230**, 895-914.

Wright, H.D., Evans, H.R. and Harding, P.W. (1987), "The use of profiled steel sheeting in floor construction", *J. Constr. Steel Res.*, **7**(4), 279-295.

Wu, Z. and Yin, J. (2003), "Fracturing behaviors of FRP-strengthened concrete structures", *Eng. Fract. Mech.*, **70**(10), 1339-1355.

Wu, L., Hoa, S.V. and Ton-That, M.-T. (2004), "Effects of water on the curing and properties of epoxy adhesive used for bonding FRP composite sheet to concrete", *J. Appl. Polym. Sci.*, **92**(4), 2261-2268.

Zhang, P., Wu, G., Zhu, H., Meng, S. and Wu, Z. (2014), "Mechanical performance of the wet-bond

interface between FRP plates and cast-in-place concrete", *J. Compos. Construct.*, **18**(6), 04014016.
Zhang, L., Wang, W., Harries, K. and Tian, J. (2015), "Bonding behavior of wet-bonded GFRP-concrete interface", *J. Compos. Construct.*, **19**(6), 04015001.

BU